

High Temperature 3D QCD: Dimensional Reduction at Work

P. Bialas^{1,2,a}, A. Morel^{3,b}, B.Petersson^{1,c}, K. Petrov^{1,d} and T. Reisz^{3,4,e}

¹Fakultät für Physik, Universität Bielefeld
P.O.Box 100131, D-33501 Bielefeld, Germany

²Inst. of Comp. Science, Jagellonian University
33-072 Krakow, Poland

³Service de Physique Théorique de Saclay, CE-Saclay,
F-91191 Gif-sur-Yvette Cedex, France

⁴Institut für Theor. Physik, Universität Heidelberg
Philosophenweg 16, D-69120 Heidelberg, Germany

Abstract

We investigate the three-dimensional $SU(3)$ gauge theory at finite temperature in the framework of dimensional reduction. The large scale properties of this theory are expected to be conceptually more complicated than in four dimensions. The dimensionally reduced action is computed in closed analytical form. The resulting effective two-dimensional theory is studied numerically both in the electric and magnetic sector. We find that dimensional reduction works excellently down to temperatures of 1.5 times the deconfinement phase transition temperature and even on rather short length scales. We obtain strong evidence that for QCD_3 , even at high temperature the colour averaged potential is represented by the exchange of a single state, at variance with the usual Debye screening picture involving a pair of electric gluons.

^apbialas@physik.uni-bielefeld.de

^bmorel@sph.t.saclay cea.fr

^cbengt@physik.uni-bielefeld.de

^dpetrov@physik.uni-bielefeld.de

^et.reisz@thphys.uni-heidelberg.de

1 Introduction

Dimensional reduction is a powerful technique to study field theories at high temperature. In the Euclidean formulation such theories are defined in a volume with one compact dimension of extent $1/T$. As the temperature T becomes large, one may expect that the non-static modes in the temperature direction can be neglected, and that one is left with a theory in one less dimension [1, 2]. This naive reduction is, however, only exact in the classical limit. In general, one has to integrate over the nonstatic modes to obtain the effective action [3, 4, 5]. As was shown in Refs [3, 5] the effective action for the long distance phenomena will, however only contain a limited number of local terms at sufficiently high temperature, because the integral over the nonstatic modes does not contain infrared divergencies. Furthermore the coefficients can be determined from a perturbative expansion of the integral over the non-static modes. This effective action is then expected to describe correctly the infrared behaviour of the full theory.

This method was first successfully applied to lattice gauge theories in Refs [5, 6, 7]. In particular the screening mass as defined from the correlation between Polyakov loops, which describes the colour averaged potential at finite temperature, was calculated. The renormalized coupling constant, used in the reduction, was defined from a perturbative calculation of this potential at small distances. In the application to pure lattice gauge theories it was possible to compare the screening length in the reduced theory with that calculated in the full theory. It was found that the dimensional reduction gave good results in the gluon plasma phase down to $T/T_c \approx 2$, where T_c is the transition temperature between the confined and the plasma phase.

The real challenge is of course the calculation in full QCD. Here the fermions can be integrated out explicitly, because they have no static modes, and they only change the coefficients in the effective action. A calculation of the screening lengths was performed in [8]. A summary can be found in [9].

Later the formalism was adapted to and successfully used to investigate the electroweak phase transition in [10]. It was also employed to determine the chromoelectric screening mass in QCD over a large range of values of the temperature [11, 12, 13]. In these articles another operator was used to define a screening mass. Also another renormalization scheme was used, the $\overline{\text{MS}}$ scheme, leading to a renormalized squared coupling around three times larger in the similar temperature range. One may thus expect higher order corrections to be more important. Further evidence for dimensional reduction in the region of a few times T_c have been found in [14], [15] and [16].

It is, of course, very interesting if several quantities can be calculated in the same scheme. In particular quantities depending on the chromomagnetic sector,

which have infrared singularities in perturbation theory that cannot be determined so far by resummation, need a non-perturbative approach. One gauge independent operator, which has been studied is the spatial string tension. However, it is still an open question what the corresponding observable is in the reduced model. In Ref. [17] it was shown that this string tension increases with the temperature in the deconfined phase. Later it was compared with the three-dimensional naively reduced theory, and a good agreement was found [18], using, however, the bare coupling constant, which even on moderately sized lattice is different from the renormalized one employed in Ref. [5] - [8].

In the present article we want to show more precisely how well dimensional reduction works, both for correlations between Polyakov loops and for the spatial string tension, in the case of three dimensional SU(3) gauge theory at high temperature. The effective model in this case is a two-dimensional Higgs model, with the Higgs field in the adjoint representation. The interest of this calculation is that the three-dimensional theory has many properties in common with the four-dimensional one, but the numerical simulations become much simpler, and one can obtain much more precise information on the quality of dimensional reduction. However, the infrared behaviour of perturbation theory is worse, so that even the leading perturbative definition of the Debye mass is not well defined. Three dimensional gauge theories at finite temperature have been considered earlier by D'Hoker [19].

In this article the three-dimensional model is investigated through numerical lattice simulations at finite temperature. Dimensional reduction is performed by perturbation theory in the static time averaged Landau gauge, using the lattice regularization, when necessary. The effective two dimensional model is also investigated by lattice simulations, which automatically include the non perturbative features of the model. A detailed comparison of correlations between Polyakov loops and of the spatial string tension is presented. Because the spatial dimension is two, we expect that the infrared properties of the theory are even more complicated than in $3 + 1$ dimensions. In particular, the Debye screening picture does not necessarily translate to QCD₃.

Our paper is organized as follows. In the next section we introduce the lattice implementation of 3-dimensional SU(3) QCD at high temperature and derive the associated dimensionally reduced model. Special care is taken in defining the self couplings of the adjoint scalar of the 2D action in the limits appropriate to the large temperature behaviour of QCD₃ in the continuum (scaling limit). Section 3 is devoted to the corresponding numerical simulations in 2 and 3 dimensions, and to the measurements of Polyakov loop correlations and spatial Wilson loops. The results are presented and discussed in Section 4. We show that the Polyakov loop correlations measured in (2+1)D or through their 2D reduction agree at large distances, and remain close to each other down to quite small distances, the more so the temperature is high. This finding gives quantitative support to the statement that,

for static observables, the reduced action correctly describes the (2+1)D properties in the limit where the momenta are small compared to temperature. The decay of these correlations with spatial distance is not compatible with the Debye screening expected from the exchange of two electric gluons, but strongly favours the existence of an isolated excitation whose mass is measured. We also show that, although the Wilson loops are non-static operators, the (spatial) string tension in (2+1)D is close to that measured in 2D, which itself differs only weakly from the known pure gauge 2D string tension. We summarize and conclude in a last section.

2 Lattice Action in 3D and its Reduction to 2D

2.1 Lattice Definitions

In this subsection we give the definitions pertinent to the simulation of SU(3) gauge theory in 2 + 1 dimensions, at finite temperature.

The gauge field action is taken to be the Wilson action on a cubic lattice Λ_3 , namely

$$S_W^3(U) = \beta_3 \sum_{x \in \Lambda_3} \sum_{\mu < \nu = 0}^2 \left(1 - \frac{1}{3} \Re \text{tr} U(x; \mu) U(x + a\hat{\mu}; \nu) U(x + a\hat{\nu}; \mu)^{-1} U(x; \nu)^{-1} \right). \quad (1)$$

The axis $\mu = 0$ is along the Euclidean time or temperature direction, and a is the lattice spacing. An SU(3) gauge group element $U(x; \mu)$ is related to the gauge fields $A_\mu^d(x)$, $d \in [1, 8]$, by

$$U(x; \mu) = \exp[i A_\mu(x)], \quad (2)$$

$$A_\mu(x) = \sum_{d=1}^8 A_\mu^d(x) \lambda^d, \quad \text{tr} \lambda^d \lambda^e = \frac{1}{2} \delta_{de}. \quad (3)$$

The λ 's denote the SU(3) algebra generators. The gauge fields are dimensionless. The lattice coupling β_3 is related to the conventional bare gauge coupling g_3 of perturbative QCD by

$$\beta_3 = \frac{6}{ag_3^2}. \quad (4)$$

The theory is super-renormalizable, g_3^2 , which has dimension one in energy, is proportional to the renormalized coupling constant squared, and can thus be used to set the physical scale. The 3D lattice action describing the system at a finite temperature T is obtained by taking for Λ_3 a cubic lattice $L_s^2 \times L_0$, and

$$T = \frac{1}{aL_0}. \quad (5)$$

The observables of interest in this work are the *spatial* string tension, as extracted from the expectation values of spatial Wilson loops formed by links $\vec{\ell}$ joining the sites $x = \vec{x} + x_0 \hat{0}$ of a rectangle $R = [R_1, R_2]$ at x_0 fixed,

$$W(R_1, R_2) = \frac{1}{3} \text{tr} \prod_{\vec{x} \in R} U(x; \vec{\ell}), \quad (6)$$

and the expectation values of Polyakov loops $L(\vec{x})$ and their connected correlations $P(\vec{x})$

$$L(\vec{x}) = \frac{1}{3} \text{tr} \prod_{x_0=1}^{L_0} U(\vec{x} + x_0 a \hat{0}, 0). \quad (7)$$

$$P(\vec{x}) = \langle L(\vec{c}) L^\dagger(\vec{c} + \vec{x}) \rangle - |\langle L(\vec{c}) \rangle|^2. \quad (8)$$

We want to study the behaviour at large T of the continuum limit of the theory defined by S_W^3 . Before proceeding, let us state more precisely what these continuum and large T limits mean in terms of the lattice parameters L_0 , β_3 and L_s . Given g_3 and T we have from (4, 5)

$$\beta_3 = \frac{6}{a g_3^2}, \quad \text{and} \quad L_0 = \frac{1}{a T}. \quad (9)$$

It follows that as $a \rightarrow 0$, scaling (constant physics) corresponds to

$$L_0 \rightarrow \infty, \quad \beta_3 \rightarrow \infty, \quad \tau \equiv \frac{\beta_3}{6L_0} = \frac{T}{g_3^2} = \text{constant}. \quad (10)$$

The dimensionless quantity τ thus measures temperature in units of the scale g_3^2 , high temperature means large τ values. From numerical simulations we obtain that $T_c/g_3^2 \approx 0.61$ [20]. Also, on the lattice, L_s must be kept much larger than the largest spatial correlation length in lattice units. Assuming that this length is of order $1/(a g_3^\alpha T^{(1-\alpha/2)})$ for some $\alpha > 0$, this together with (5) implies

$$\frac{L_s}{L_0} \gg \left(\frac{\sqrt{T}}{g_3} \right)^\alpha = \sqrt{\tau}^\alpha. \quad (11)$$

Note that this ratio increases with temperature. As we shall see, these considerations, important for the design a meaningful numerical investigation of the high temperature phase of QCD₃, are also useful to discuss the adequacy of its 2D reduction to describe at least part of its large distance physics.

2.2 Dimensional Reduction: the Effective 2D Action

The dimensional reduction means that one should derive an effective action for the static modes, obtained by keeping the static part of the action and adding terms coming from a perturbative integration over the non-static modes. It is therefore convenient to choose a static gauge, where this separation can be made.

The operators of interest to us are gauge invariant and may be computed in any gauge. In particular, a static gauge can be realized on the lattice with periodic boundary conditions by choosing A_0 independent of the imaginary time coordinate x_0 :

$$A_0(x_0, \vec{x}) = A_0(\vec{x}). \quad (12)$$

In such a gauge the Polyakov loops are static operators, unlike spatial Wilson loops, and read

$$L(\vec{x}) = \frac{1}{3} \text{tr} \exp[i L_0 A_0(\vec{x})]. \quad (13)$$

Full gauge fixing, which is necessary for forthcoming perturbative calculations [21], is achieved by adding the Landau constraint

$$\sum_{x_0} \sum_{i=1}^2 [A_i(x) - A_i(x - \hat{a}_i)] = 0. \quad (14)$$

Together with (12), this condition constitutes the so-called static, time-averaged Landau gauge (STALG, see [22, 23]).

At high temperature and in the thermodynamical limit, the well known Z_3 symmetry of the S_W^3 action is broken (deconfined phase) and the average Polyakov loop $\langle L(\vec{y}) \rangle$ is not zero. Its phase may be either one of the three 3^{rd} roots of one, the corresponding threefold degeneracy can be lifted up by rotating this phase away, so that the U 's are always connected to the unit matrix.

In what follows, then, the gauge manifold will be parametrized by gauge fields $A_\mu^d(x)$ subjected to the constraints (12, 14), and perturbation theory, whenever it applies, is generated by expanding the 3D action into small fields.

The effective 2-dimensional action is obtained according to standard techniques ([1]-[5]). It consists in the classically reduced 3D action, with *all fields* restricted to their static components (no dependence in the 0^{th} coordinate), supplemented by the interactions generated by integrating over the non-static degrees of freedom which are left over after gauge fixing, namely the non-static part $A_i^{ns}(x_0, \vec{x})$, $i=1,2$, of the gauge fields, constrained by (14). The resulting action depends on the 2-dimensional SU(3) gauge fields $A_i^{static}(\vec{x})$ defined by

$$A_i(x) = A_i^{static}(\vec{x}) + A_i^{ns}(x_0, \vec{x}), \quad (15)$$

$$\sum_{x_0} A_i^{ns}(x_0, \vec{x}) = 0, \quad (16)$$

and on $A_0(\vec{x})$, a scalar in 2 dimensions (Higgs field in the adjoint representation). In the following, the superscript *static* on the 2D gauge fields will be omitted. So defined, this action is of course non polynomial and non local in A_0 .

At large T however, one may truncate its expansion in powers of $A(\vec{x})$, adapting the method developed in details in [5] for the 4D→3D reduction. In the present case, power counting and Becchi-Rouet-Stora symmetry of the gauge fixed theory leads to retain only the 1-loop contribution of the non-static modes to the quadratic and quartic A_0 self-couplings at external momenta $p = 0$. The contributions of monomials of higher degree, or non local in A_0 are suppressed by powers of $(g_3^2/T)^2$ and $(p/T)^2$, up to log's. More precise statements will be made at the end of this section.

We write down the explicit result S_{eff}^2 of this reduction, in terms of the parameters L_0 and β_3 of the initial 3D lattice action (L_s is assumed to satisfy (11) so that finite size effects are negligible).

For later convenience, we rescale the scalar field by setting

$$A_0(\vec{x}) = \phi(\vec{x}) \sqrt{\frac{6}{L_0 \beta_3}}, \quad (17)$$

and express S_{eff}^2 as a function of ϕ and of the 2-dimensional U 's. It contains three pieces, a pure gauge part S_W^2 , the gauge covariant kinetic term $S_{U,\phi}$ for ϕ , and the self-interaction S_ϕ induced by integration over the non static fields:

$$S_{eff}^2(U, \phi) = S_W^2 + S_{U,\phi} + S_\phi. \quad (18)$$

Here S_W^2 is the Wilson action for $D = 2$ obtained by repeating L_0 times the purely spatial part of S_W^3 . Hence

$$S_W^2 = \beta_2 \sum_{\vec{x} \in \Lambda_2} \left(1 - \frac{1}{3} \Re \text{tr} U(\vec{x}; 1) U(\vec{x} + a\hat{1}; 2) U(\vec{x} + a\hat{2}; 1)^{-1} U(\vec{x}; 2)^{-1} \right), \quad (19)$$

$$\beta_2 = \beta_3 L_0. \quad (20)$$

The lattice kinetic term for the (adjoint) field ϕ is obtained by expanding the S_W^3 action to second order in A_0 , and reads

$$S_{U,\phi} = \sum_{\vec{x}} \sum_{i=1}^2 \text{tr} \left(D_i(U) \phi(\vec{x}) \right)^2, \quad (21)$$

$$D_i(U) \phi(\vec{x}) = U(\vec{x}; i) \phi(\vec{x} + a\hat{i}) U(\vec{x}; i)^{-1} - \phi(\vec{x}). \quad (22)$$

Finally the ‘‘Higgs potential’’ S_ϕ is written

$$S_\phi = \sum_{\vec{x}} h_2 \text{tr} \phi(\vec{x})^2 + h_4 \left(\text{tr} \phi(\vec{x})^2 \right)^2. \quad (23)$$

In the scaling limit (10) explained in subsection 2.1, we drop those terms of the small a expansion of h_2/a^2 and h_4/a^2 which vanish as $a \rightarrow 0$ and find

$$h_4 = \frac{9}{16\pi\beta_3^2}, \quad (24)$$

$$h_2 = -\frac{9}{\pi L_0 \beta_3} \left(c_0 \log L_0 + c_1 \right); \quad c_0 = 1, \quad c_1 = \frac{5}{2} \log 2 - 1. \quad (25)$$

We call these expressions the scaling parts of h_2 and h_4 . Let us sketch how these results have been derived and comment on them.

The coupling h_4 requires the 1-loop nonstatic contribution to the Green's function $\tilde{\Gamma}_{ns}^{(4)}(\vec{p} = \vec{0})$ with four external A_0 fields at zero momentum. At $T = 0$, the Feynman integrals involved in the continuum all are of the type $\int d^3k/k^4$ and thus UV convergent but IR divergent. At $T \neq 0$, the restriction to non static modes ($k_0 \neq 0$) makes them IR finite. For these reasons, h_4 can be, and was, calculated directly in the continuum. Our result (24) coincides with that obtained by adapting to $D = 3$ the calculation of Nadkarni [3] for $D = 4$.

The case for h_2 is slightly more tricky. It is given by

$$h_2 = -\frac{6}{\beta_3} \tilde{\Pi}_{00}^{ns}(0), \quad (26)$$

where $\tilde{\Pi}_{00}^{ns}(0)$ is the 1-loop contribution of the non static modes to the vacuum polarization at zero momentum. Two Feynman graphs contribute, with one and two A_i internal propagators, respectively of the form $g_3^2 \int^\Lambda d^3k/k^2$ and $g_3^2 \int^\Lambda d^3k k_0^2/(k^2)^2$, both linearly divergent with the cut-off Λ . However, at $T = 0$, gauge invariance guarantees $\tilde{\Pi}_{00}(0) = 0$, so that the two graphs cancel each other exactly there. At $T \neq 0$, the cancellation is only partial, still leaving a logarithmic UV divergence. We thus computed $\tilde{\Pi}_{00}^{ns}(0)$ *on the lattice*, which provides a cut-off of order $\Lambda \simeq 1/a = T L_0$ at high temperature according to Eq.(5), hence the $\log(L_0)$ term in (25).

Applying the Feynman rules of [24], the finite lattice expression of $\tilde{\Pi}_{00}^{ns}(0)$ is found to be

$$\tilde{\Pi}_{00}^{ns}(0) = \frac{3}{L_0 L_s^2} \sum_{k_0 \neq 0} \sum_{\vec{k}} \left\{ \frac{2c_{k_0}^2 \hat{k}_0^2}{(\hat{k}^2)^2} - \frac{1 - \hat{k}_0^2/2}{\hat{k}^2} \right\}, \quad (27)$$

$$\hat{k}_\mu = 2 \sin(k_\mu/2), \quad \hat{k}^2 = \sum_0^2 \hat{k}_\mu^2, \quad c_{k_\mu} = \cos(k_\mu/2). \quad (28)$$

The $L_s \rightarrow \infty$ limit is obtained by the replacement $(2\pi/L_s)^2 \sum_{\vec{k}} \rightarrow \int_{-\pi}^{\pi} d^2k$. After

some manipulations, one arrives at

$$\tilde{\Pi}_{00}^{ns}(0) = \frac{3}{L_0} \sum_{n_0=1}^{L_0-1} \left(-\frac{1}{2}(1-2t)S(t) - t(1-t)\frac{dS(t)}{dt} \right), \quad t = \sin^2\left(\frac{\pi n_0}{L_0}\right), \quad (29)$$

$$S(t) \equiv \frac{1}{4\pi^2} \int_{-\pi}^{\pi} \frac{dk_1 dk_2}{2(1+t) - \cos(k_1) - \cos(k_2)}. \quad (30)$$

It is clear on the latter equation that $S(t)$ has a logarithmic singularity at $t = 0$. The result (25) follows from (26) after the asymptotic behaviour at large L_0 and infinite L_s of $\tilde{\Pi}_{00}^{ns}(0)$ is inserted. Details on its derivation from (29) are given in the appendix. Here, we just mention a useful trick used to evaluate $\tilde{\Pi}_{00}^{ns}(0)$, noting that Eq.(29) can be rewritten as

$$\tilde{\Pi}_{00}^{ns}(0) = -\frac{3}{2L_0} \sum_{n_0=1}^{L_0-1} \frac{d}{dx} G(x), \quad x = \frac{\pi n_0}{L_0}, \quad (31)$$

$$G(x) \equiv \sin x \cos x S(\sin^2 x). \quad (32)$$

At large L_0 , $\sum_{n_0=1}^{L_0-1} \frac{d}{dx} G(x)$ is of order $L_0/\pi \int_{\pi/L_0}^{\pi-\pi/L_0} dG(x) = -2L_0/\pi G(\pi/L_0)$: The linear divergence in L_0 is cancelled by the $\sin(\pi/L_0)$ factor in G while the $\log L_0$ originates from the logarithmic behaviour of $S(\sin^2 x)$ at $x \simeq \pi/L_0$.

2.3 About the Reduced Action: Summary and Remarks

We first summarize what has been done above. The QCD₃ lattice action is given by Eq.(1). The parameters of physical relevance are the lattice coupling β_3 and L_0 . The observables we consider are the Polyakov loops (7) and their correlation (8), and the spatial Wilson loops (6).

Dimensional reduction leads to the 2D lattice effective action described by Eqs. (18-25). It is a gauge invariant model for a scalar ϕ in the SU(3) adjoint representation, whose ‘‘Higgs potential’’ is truncated at order 4 in ϕ at high temperature and low momenta. The lattice gauge coupling and scalar self couplings β_2, h_2 and h_4 are fixed by the 3D parameters Eqs. (20, 25, 24). The Higgs field is normalized in such a way its kinetic term in the classical limit is $\text{tr}(\partial_i \phi)^2$.

Let us now comment upon what we have obtained. First, as announced before, it is consistent to truncate the effective action to order ϕ^4 , with h_2 and h_4 couplings computed at 1-loop order. To be more precise, power counting and inspection show that h_n/a^2 , with h_n the coupling associated with any monomial of degree n in ϕ , has the following order of magnitude:

$$n = 2 \quad : \quad g_3^2 T + g_3^2 T \log T \left(1 + \mathcal{O}[(p/T)^2, g_3^2/T] \right), \quad (33)$$

$$n = 4 : \quad g_3^4 (1 + \mathcal{O}(g_3^2/T)), \quad (34)$$

$$n \geq 6 \text{ even} : \quad O(T^2 (g_3^2/T)^{n/2}), \quad (35)$$

$$n \geq 3 \text{ odd} : \quad O(T^2 (g_3^2/T)^{n/2} (p/T)). \quad (36)$$

The corrections for $n = 2$ and 4 come from 2-loop order and non-local effective interactions. It is thus consistent to neglect the $n = 6$ and higher power monomials, as well as all couplings with n odd, and to keep h_2 as given by Eq. (25).

We next note that unlike h_4 which is positive, insuring boundedness of the partition function at large fields, the quadratic coupling h_2 is negative. The “potential” thus have a shape typical for gauge symmetry breaking by Higgs mechanism. Of course, this symmetry breaking is not expected to occur in 2 dimensions. In fact, the form (25) of this coupling can be seen as a counterterm for the logarithmic UV divergence of the 2D model, here prescribed in advance by the UV regularization of the 3D model, while the actual IR behaviour of the theory is highly non perturbative.

In the static gauge chosen, the 3D Polyakov loop operator is given in 2 and 3 dimensions by the same function (13) of the A_0 field. According to the normalization (17) of the ϕ field and to Eqs. (10, 20), it reads

$$L(\vec{x}) = \frac{1}{3} \text{tr} \exp(i \phi(\vec{x}) / \sqrt{\tau}), \quad (37)$$

$$\tau = \frac{\beta_3}{6L_0} = \frac{\beta_2}{6L_0^2} = \frac{T}{g_3^2}. \quad (38)$$

Along a line $\tau = \text{const.}$ (constant physics, see subsection 2.1), the operator used to probe dimensional reduction remains unchanged, and it is thus consistent to compare the Polyakov loop correlations measured in 3 and 2 dimensions at the same fixed τ value. The continuum limit is $L_0 \rightarrow \infty$, and constant (large distance) physics at large L_0 can be checked within either one of the two models.

Let us then consider the effective action S_{eff}^2 in terms of the dimensionless temperature τ , Eq. (38), and of the lattice parameter L_0 . After setting $a^2 g_2^2 = 6/\beta_2$, and using Eqs. (20, 25, 24, 38), the three dimensionless couplings $(ag_2)^2$, h_2 and h_4 read

$$(ag_2)^2 = \frac{1}{\tau L_0^2}, \quad (39)$$

$$h_2 = -\frac{3}{2\pi} \frac{c_0 \log L_0 + c_1}{\tau L_0^2}, \quad (40)$$

$$h_4 = \frac{1}{64\pi} \frac{1}{\tau L_0^2} \frac{1}{\tau}. \quad (41)$$

We see that, except for the $\log L_0$ in h_2 , these three couplings all scale as $1/L_0^2$ with L_0 , while as a function of τ , h_4 is τ times smaller than the two other ones.

Let us finally write down the effective Lagrangian \mathcal{L}_{eff} , as obtained from the small a expansion of the effective action S_{eff}^2 . In S_{eff}^2 , we make the substitution $A_i \rightarrow ag_2 A_i$, replace $\sum_{\vec{x}}$ by $a^{-2} \int d^2x$, use T and g_2^2 as parameters instead of the lattice β_3 and L_0 , and take the limit $a \rightarrow 0$ (but in $\log L_0 \equiv -\log aT$ in the ϕ^2 term). We obtain

$$\mathcal{L}_{eff} = \frac{1}{4} \sum_{c=1}^8 F_{ij}^c F_{ij}^c + \text{tr} [D_i \phi]^2 + \frac{g_2^2}{32\pi} \left(\frac{g_2}{T} \right)^2 \text{tr} \phi^4 + \mathcal{L}_{CT}, \quad (42)$$

$$D_i \phi = \partial_i \phi + ig_2 [A_i, \phi],$$

$$F_{ij} = \partial_i A_j - \partial_j A_i + ig_2 [A_i, A_j],$$

$$\mathcal{L}_{CT} = -\frac{3g_2^2}{2\pi} \left[-\log(aT) + 5/2 \log 2 - 1 \right] \text{tr} \phi^2. \quad (43)$$

This is a 2D, SU(3) gauge invariant Lagrangian for an adjoint scalar ϕ , but it is far from being the most general one. The gauge coupling g_2 , with its canonical dimension one in energy, sets the scale. The non kinetic quadratic term is the counterterm \mathcal{L}_{CT} , suited to a lattice UV regularization with spacing a . The quartic self interaction $\lambda_4 = g_2^2 \times (g_2/T)^2$, generically a free parameter, here goes to zero as $T \rightarrow \infty$ in units of g_2 , and presumably plays a marginal role. We also note the absence in the model of odd powers ϕ^{2k+1} , allowed by gauge symmetry for $k > 0$. The corresponding Z_2 symmetry might however be spontaneously broken in some subspace of the unrestricted parameter space g_2, h_2, h_4 . The similar problem in $4 \rightarrow 3$ QCD reduction has been studied in Ref. [12]. For the case of SU(2) in (3+1)D, Z_2 is the center of the gauge group so that Z_2 breaking is also gauge symmetry breaking, a subject previously discussed in Refs. [25], [26] and [11].

3 The Numerical Simulations in (2+1) and 2 Dimensions

We simulated the reduced theory using the same method as in reference [7]. For updating the gauge fields U we employed a mixed algorithm, where new trial SU(3) matrices were generated by the heath–bath algorithm and are accepted according to a Metropolis condition on the hopping term. We used the standard Cabibbo–Marinari pseudo heath–bath algorithm based on updating the SU(2) subgroups of a SU(3) matrix [27]. The new SU(2) sub–matrices were generated using the Kennedy–Pendleton algorithm [28]. After each subgroup update the resulting matrix was subjected to the Metropolis question on the hopping term. This approach results in an acceptance rate close to 95%.

Alternatively we tried the multi-hit Metropolis algorithm. An update of a single link variable was attempted several times (typically eight) before attempting to update next variable. The trial matrices were generated according to $U \rightarrow \exp(iA)U$ where A was an hermitian matrix generated from the distribution $\exp(-\epsilon \text{tr} A^2)$. The parameter ϵ was tuned to obtain the acceptance ratio around 50%. Because generation of trial matrices is expensive in CPU time (matrix exponentiation) we took the values from a table that was regenerated every five sweeps. The autocorrelation times for this algorithm were comparable to the heath-bath but the CPU time required to perform a metropolis update was approximately two times bigger.

The scalar fields were updated using the multi-hit metropolis. At every point we tried typically eight updates. New scalar fields were obtained from $A \rightarrow A + \delta A$ where δA was generated according to $\exp(-\epsilon \text{tr} A^2)$. For each set of coupling constants, ϵ was tuned to obtain the acceptance ratio around 50%. One sweep over the lattice consisted of one update of gauge fields followed by one update of scalar fields. After each sweep we measured “control” variables : expectation value of plaquette, $\text{tr} A^2$, $\text{tr} A^3$ and $\text{tr} A^4$.

All runs except for scaling test (see the next section) were performed on 32×32 lattices with the parameter L_0 set equal to 4. The dynamics of the gauge and Higgs sectors turned out to be quite different. The integrated autocorrelation time of the plaquette operator was typically non-measurable ($\lesssim 1$) while for $\text{tr} A^2$ it varied between 100 and 400 sweeps when β_3 was varied from 21.0 to 346.0. For each value of β we have collected typically 10^6 sweeps.

In three dimensions we used the data previously gathered on the Quadrics APE supercomputer [20] on $32 \times 32 \times 4$ lattices.

The main quantities measured were the average $\langle L(\vec{x}) \rangle$ of the Polyakov loops, their on-axis 2-body correlations $P(r)$, and the average $\langle W(R_1, R_2) \rangle$ of spatial Wilson loops. In three dimensions they are defined by (6), (7) and (8). The only difference in two dimension is that the Polyakov loop is given by (13). When necessary, an index $D = 2 + 1$ or 2 specifies the dimension considered. Both 2D and 3D data were analyzed in the same way as to minimize the systematic errors.

In 2D simulations Wilson loops were measured every ten sweeps and blocked by 50. Integral autocorrelation time for the measurements of 14×14 Wilson loops was, in the worst case, of the order of one and was negligible in the majority of cases. The measurement routine is quite expensive and consumed almost half of the CPU time.

In order to extract the string tension, local potentials were first extracted from the ratios :

$$V(R, R') = \log \frac{\langle W(R, R') \rangle}{\langle W(R, R' + 1) \rangle}. \quad (44)$$

By definition, the potential is

$$V(R) = \lim_{R' \rightarrow \infty} V(R, R'). \quad (45)$$

For each given R , $V(R, R')$ was found to decay exponentially to a constant in R' . In practice, the constant regime is reached within errors above $R' = 3$ and the potential was fitted in the range $R' \in [4, 12]$. The string tension σ was then obtained from the ansatz

$$V(R) = V_0 + \sigma R. \quad (46)$$

A fit to the above linear potential is sufficient to obtain a stable value of σ within errors when it is performed in the range from $R_{min} = 2$ to R_{max} . The R_{max} values, depending upon the value of β_3 , varied from 10 to 14. The χ^2 value in the 3D case was of the order of one, and about ten times less in the 2D case, likely due to large correlation between points.

The errors on σ were calculated by the triple application of the jack-knife method. In order to calculate the jack-knife estimate of the error on σ from the fit to the formula (46) we used 16 jack-knife copies of the potential $V(r)$ with errors. To estimate the errors of every copy we applied the jack-knife algorithm with the same block size again to each of the corresponding 16 data sets, thus generating 15 copies of every set. However, in order to calculate the $V(r)$ we needed the ratios $V(R, R')$ again with errors. Calculation of these errors was done by a third and last jack-knife step applied to each of 16×15 data sets obtained in the previous step.

Polyakov loops correlators were also measured every ten sweeps. While, due to the large auto-correlation time, this was in a sense an “oversampling”, it did not take much of the CPU time. The measurements were blocked by 50 and then written out. Afterwards the data were again blocked into 25 blocks. These 25 blocks were used to calculate the connected correlators with errors estimated by jack-knife algorithm. We also tried different numbers of blocks and did not observe any significant change in the results. The double jack-knife algorithm, similar to the one described for the Spatial Wilson loops, was used to estimate the error for fits of the connected correlator to the formulae (49, 50) used to extract a screening length (see next section). The fits were done in the interval $r \in [r_{min} = 4, 15]$. We have checked that varying r_{min} from 3 to 6 does not change the results.

4 Results and Discussion

We now present our results, discussing successively dimensional reduction (how well does the effective 2D model describe quantitatively the large distance physics of high temperature QCD₃), scaling (is the parameter region explored close to the continuum limit), the screening length in the Polyakov loop channel and the spatial string tension.

4.1 Dimensional Reduction

Let us compare the Polyakov loop correlations $P_{2+1}(r)$ extracted from Ref. [20] and $P_2(r)$ measured in our simulation. A conservative statement on dimensional reduction is to say that the lowest physical state coupled to $L(\vec{x})$ is the same in both cases, so that the two functions must have the same *shape* in r at large r . A stronger statement is that, to the extent that the weight associated with S_{eff}^2 is a good approximation to the integral over the non-static fields of the $(2+1)D$ weight, in the small p/T regime at least, the averages with respect to the two weights of a static operator such as $\langle L(\vec{x}) L(\vec{y}) \rangle$ are *equal* at large $|\vec{x} - \vec{y}|$. We will show that this latter situation is indeed approached at large enough temperature.

We recall that temperature is given in units of the gauge coupling by

$$\tau \equiv \frac{T}{g_3^2} = \frac{\beta_3}{6L_0}. \quad (47)$$

Using $L_0 = 4$ fixed, we investigate the temperature dependence of the correlations by varying β_3 in the range [21, 173]. High temperature means β_3 sufficiently larger than the transition point in $(2+1)D$, which was found to occur at $\beta_c = 14.73$ for $L_0 = 4$ [20].

Fig.1 compares the correlations $P_{2+1}(r)$ and $P_2(r)$ for $\beta_3 = 29$ and 84. The curves are fits of the $P_2(r)$ function, to be explained below. We see that the two correlations are extremely close one to the other: not only they have the same *shape* at large r , which is the primary prediction of dimensional reduction, but also nearly the same *normalization*. As announced, this finding favours dimensional reduction in the strong sense. In addition, we notice that this agreement between the two ways of computing the Polyakov loop correlation extends down to fairly small values of r . Since the normalization is set by $|\langle L(\vec{x}) \rangle|^2$, it shows that, although it is local, the Polyakov operator is not very sensitive to the short wave length terms omitted in the effective action. That it is the case is born out by the data of Table 1, where our results for $\langle L_2(\vec{x}) \rangle$ and $\langle L_{2+1}(\vec{x}) \rangle$ are presented. Relatively to their distance to one (their common value at $\beta_3 = \infty$), their difference, already $\sim 6\%$ at $\beta_3 = 21$, decreases to $\sim 0.6\%$ at $\beta_3 = 173$.

In Fig. 2, we illustrate more in details, for the β_3 values not reported on in Fig. 1, how well the $2D$ and $(2+1)D$ correlations compare. Their ratio P_{2+1}/P_2 is plotted against the distance r in lattice units. These data definitely support the statement that P_{2+1}/P_2 remains quite flat and close to one in the whole r and T range. Recalling that the lowest T value is only ~ 1.5 times T_c , and that the correlation functions decrease in r by about three orders of magnitude, we conclude that the effective local $2D$ action reproduces the $(2+1)D$ Polyakov loop correlations with a remarkable accuracy, soon above the transition, and down to distances even shorter than $1/T$.

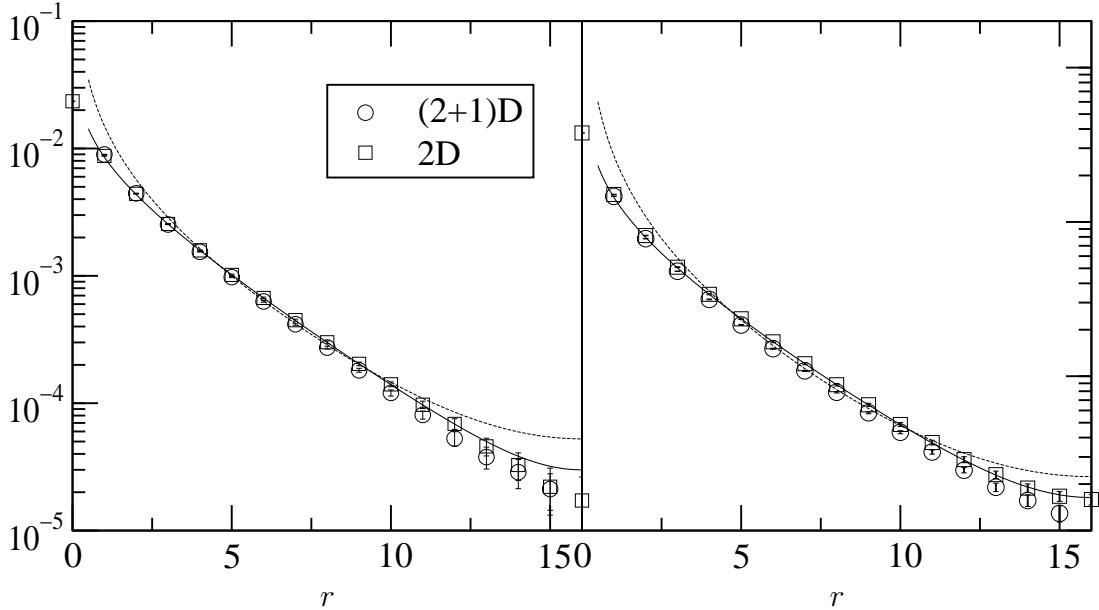


Figure 1: Polyakov Loop Correlations $P_D(r)$, $D = 2 + 1$ (circles) and 2 (squares), for β_3 equal to 29 (left) and 84 (right). Distance r is given in lattice units. In both cases $L_s = 32$ and $L_0 = 4$. The 2D data were produced using h_2 from Eq. (25). The continuous and the dashed lines result respectively from fitting formulae (49) and (50) to the 2D data.

4.2 Scaling

Given the temperature, the continuum limit is approached by taking

$$\tau = \frac{\beta_3}{L_0} = \frac{T}{g_3^2} \quad \text{fixed}, \quad L_0 = \frac{1}{aT} \quad \text{large}. \quad (48)$$

Scaling is thus the statement that, at fixed τ , the physics do not change with L_0 , if L_0 is large enough. We checked that by comparing the Polyakov loop correlations in 2D for two sets of lattice parameters, namely $[\beta_3, L_0, L_s] = [29, 4, 32]$ and $[58, 8, 64]$. Given T , doubling L_0 means dividing the lattice spacing a by two, so that the *physical* spatial size aL_s of the lattice is unchanged. The resulting correlations are presented in Fig. 3 showing a very similar shape as a function of the physical distance. It is again instructive to consider their ratio, found to be quite flat at all distances (Fig. 4): Within errors, there is no sizable deviation from scaling. Note that this constant ratio is not one. It is given by that of the corresponding values of $|\langle L(\vec{x}) \rangle|^2$, which is not a physical quantity (remember that the 2D effective Lagrangian contains an explicit (logarithmic) dependence on a via its counterterm Eq. (43)).

β_3	$ \langle L_2(\vec{x}) \rangle $	$ \langle L_{2+1}(\vec{x}) \rangle $
21.0	0.56002 (62)	0.53467 (16)
29.0	0.67007 (25)	0.66120 (13)
42.0	0.76397 (20)	0.76130 (12)
84.0	0.87392 (11)	0.87435 (6)
173.0	0.93494 (13)	0.93530 (11)

Table 1: The average Polyakov loop as a function of β_3 in (2+1)D and 2D.

Hence scaling is verified in the range of interest. It justifies keeping $L_0 = 4$, which is less expensive in computer time and allowed us to use the existing data of [20] in $(2 + 1)D$.

4.3 Screening Lengths

The fast decay with r of the correlation functions is consistent with the existence of a finite spatial correlation length, ξ_S , associated with the quantum numbers of the Polyakov loop operator, a colour singlet scalar. A mass can be defined as usual by $M_S = \xi_S^{-1}$. In the similar situation with one more dimension, perturbation theory is invoked to state that M_S is $2M_E$, twice the so called electric screening mass, because the lowest “state” coupled to the loop is a two electric gluon state. If this is so, the $P(r)$ correlation is expected to be proportional at large r to the square of the correlation function for a one particle state of mass M_E . In the present case however, the infrared sector is more complicated and perturbation theory is doubtful. In particular we let open the possibility that there exists in the PL channel an independent screening mass M_S , associated with a true thermal excitation of the $2D$ system. In the latter case, we parametrize the data according to

$$P_D^{(m_S)}(r) \simeq c \left(\frac{1}{[m_S r]^{1/2}} e^{-m_S r} + \frac{1}{[m_S (L_s - r)]^{1/2}} e^{-m_S (L_s - r)} \right), \quad (49)$$

while in the former case one rather expects

$$P_D^{(2m_E)}(r) \simeq c' \left(\frac{1}{[m_E r]^{1/2}} e^{-m_E r} + \frac{1}{[m_E (L_s - r)]^{1/2}} e^{-m_E (L_s - r)} \right)^2. \quad (50)$$

The m symbols denote masses in lattice units, i.e. $m \equiv aM$. These parametrizations respect the lattice symmetry $r \rightarrow L_s - r$. Since we have no direct access to m_E , the two above expressions differ in shape through the prefactors, $r^{-1/2}$ and r^{-1}

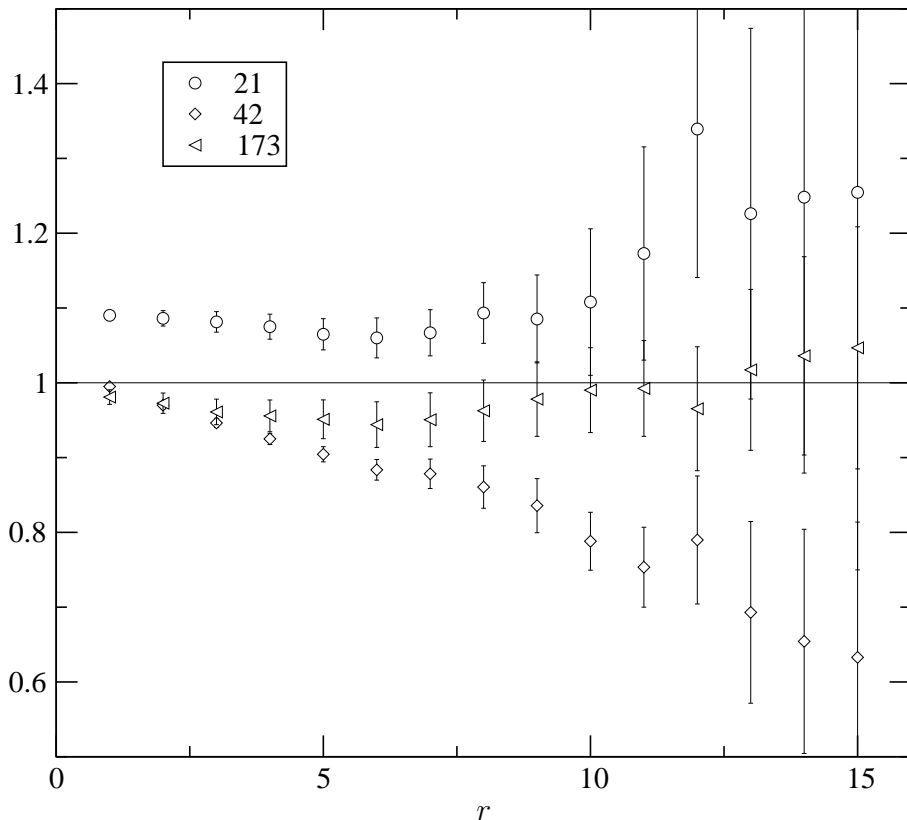


Figure 2: Ratios $P_{2+1}(r)/P_2(r)$ of Polyakov Loop correlations as functions of the lattice distance r for $\beta_3 = 21, 42, 173$.

respectively. We checked that for $r > 1$, lattice artefacts are negligible in the mass range considered. This was achieved by comparing Eq. (49) to the lattice propagator

$$P_{Latt}(m_S, r) = \frac{1}{L_s^2} \sum_{p_1, p_2} \cos(p_1 r) \tilde{P}_{Latt}(m_S, \vec{p}), \quad (51)$$

$$\tilde{P}_{Latt}^{-1}(m_S, \vec{p}) = \tilde{p}^2 + 4 \sinh(m_S^2/4). \quad (52)$$

in the notations of Eq. (28). We carefully analyzed our numerical data, and *we find that the ansatz (49) is by far the best one*, giving a good fit of the data down to small r values. For illustration, the continuous curves of Fig. 1 are fits of the form (49) to $P_2(r)$, $r \geq r_{min}$, with $r_{min} = 4$, and changing r_{min} from 3 to 6 does not change the answer for m_S within errors. The only deviation which we observe is at (very) short distances, where some more massive contribution may be present, if not an artefact of the lattice UV regularization. It is anyway too small to be reliably analyzed. On the contrary, fits to the same data of the form Eq. (50) lead in Fig. 1

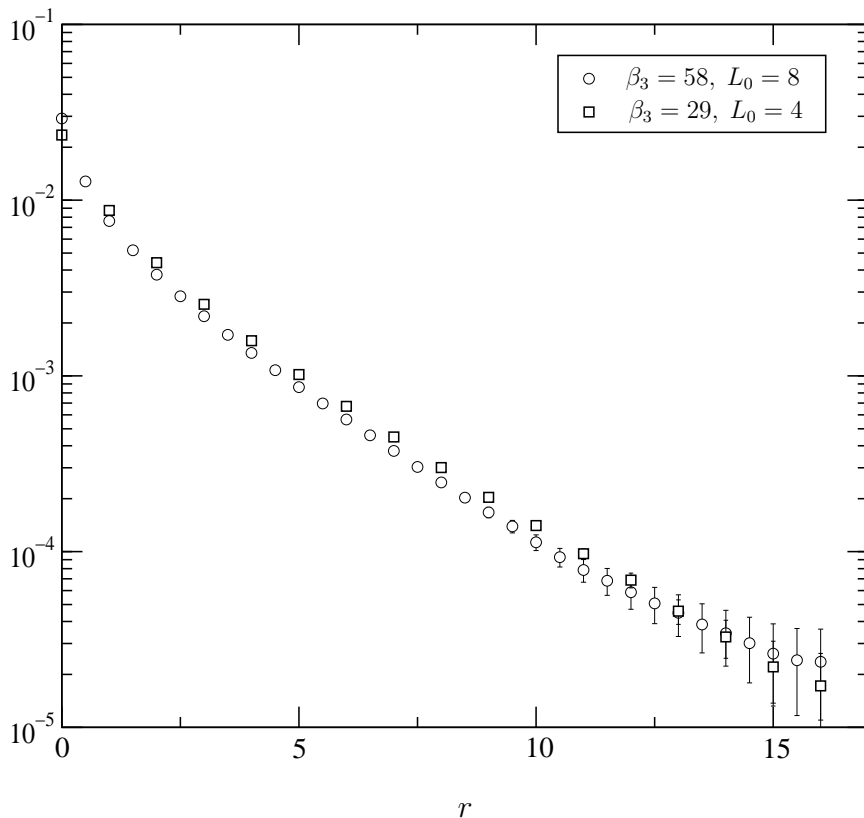


Figure 3: Comparison of the Polyakov Loops Correlations in the 2D model for the two sets of parameters $[\beta_3, L_0, L_s] = [29, 4, 32]$ and $[58, 8, 64]$ i.e. for constant τ (10). The values of r for $L_0 = 8$ (circles) are scaled down by a factor two in order to maintain the same physical scale.

to the dashed curves, which are clearly not acceptable. The results of systematic fits of expression (49) to all available correlations $P_2(r)$ and $P_{(2+1)}(r)$ are presented in Fig.5. The corresponding dimensionless quantities $M_S/(g_3\sqrt{T}) \equiv m_S\sqrt{L_0\beta_3/6}$ are plotted versus $g_3^2/T \equiv 6L_0/\beta_3$. Also shown for comparison are the masses resulting from a few simulations made with the so-called naive effective action ($h_2 = h_4 = 0$). The latter are far away from the former, showing the important effect of taking into account the non static degrees of freedom. We also made runs where, instead of using the so-called scaling form (25) of h_2 , we took the value obtained numerically from Eqs. (26, 28). The results are similar, especially at high temperature, but anyway distinguishable within our statistical accuracy. This shows a great sensitivity of the static properties to the quadratic counterterm (43), an interesting feature per se.

The scaling properties observed in subsection 4.2 of course reflect themselves

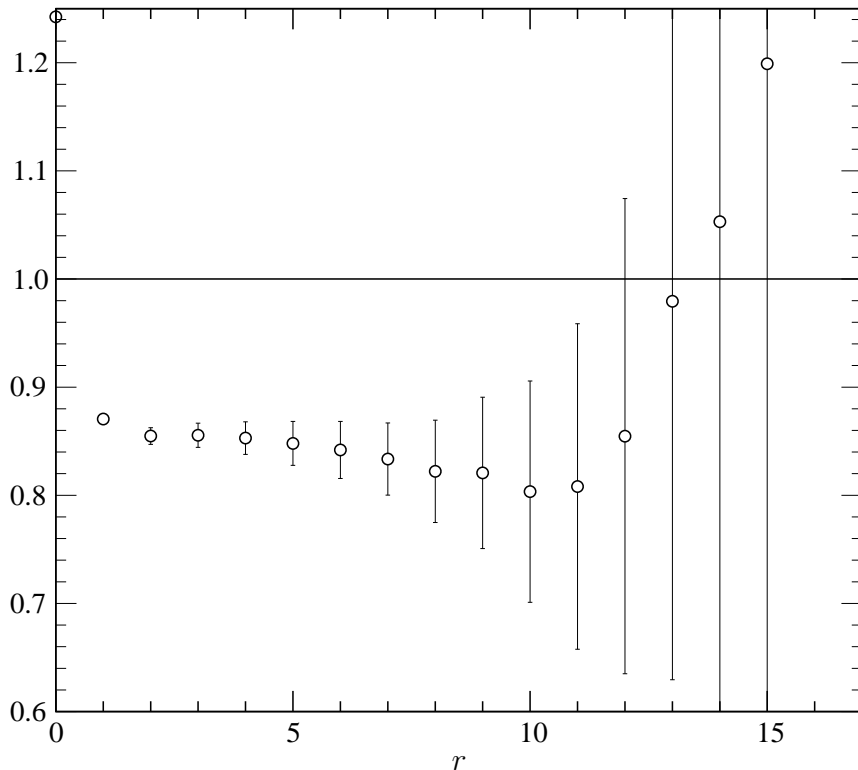


Figure 4: The ratio between the two Polyakov loop correlation functions presented in figure 3.

in the mass values. For the two cases compared there, we find $M_S a = 0.331(6)$ and $0.169(3)$: the lattice spacing is reduced exactly by two within errors.

Of course the fact that dimensional reduction works well for masses directly follows from its success for correlations. We preferred to illustrate it first on the lattices, as done in Fig.2, that is independently of any interpretation of the nature of the observed screening lengths. What we now get in addition is that the main signal observed in the Polyakov loop channel favours the existence of a true colour singlet excitation of the high temperature gluon system, rather than it reflects the existence of an electric screening length (Debye screening) in the one longitudinal gluon channel.

4.4 The Spatial Wilson Loop

The spatial Wilson loop W in 3D is not a static operator, and thus not predicted to assume the same value at high temperature and in the 2D reduced model. However i) a non zero spatial string tension σ_{2+1} is known to exist [20] above the deconfinement temperature, ii) the pure gauge 2D theory is confining and produces a string tension

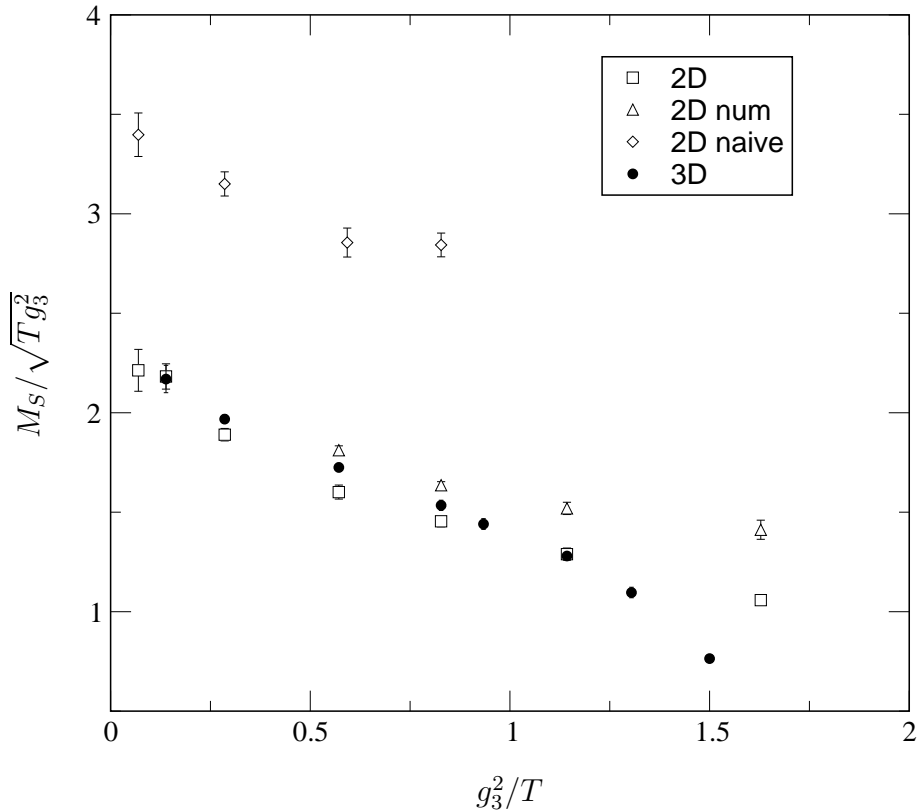


Figure 5: Physical screening masses M_S in units of $g_3\sqrt{T}$ versus g_3^2/T , in $(2+1)D$ (black points) and $2D$ (squares). Also shown are the masses obtained with the numerical value of h_2 from Eq. (26) (triangles) instead of its asymptotic expression (25), and with the “naive” reduced action: no Higgs potential, $h_2 = h_4 = 0$.

σ_2^0 [29], and iii) in two dimensions we expect confinement and thus a finite string tension σ_2^ϕ to survive when the Higgs field ϕ is turned on.

It is thus interesting to compare these three quantities as a function of the temperature of the $(2+1)D$ model. For this comparison, we take $a^2\sigma_{2+1}$ and $a^2\sigma_2^\phi$ from the analysis of W data provided by [20] and by our simulation, whereas $a^2\sigma_2^0$ is computed analytically at large $\beta_2 = L_0\beta_3$. This is obtained by expanding in $1/\beta_2$ the one plaquette $SU(3)$ partition function (Eq. (19) for one single site). The $SU(3)$ integral is performed following [30], and one finds

$$a^2\sigma_2^0 = \frac{4}{\beta_2} + \frac{7}{\beta_2^2} + \mathcal{O}(\beta_2^{-3}). \quad (53)$$

The next terms are easy to derive, but not required for our purpose. This expression

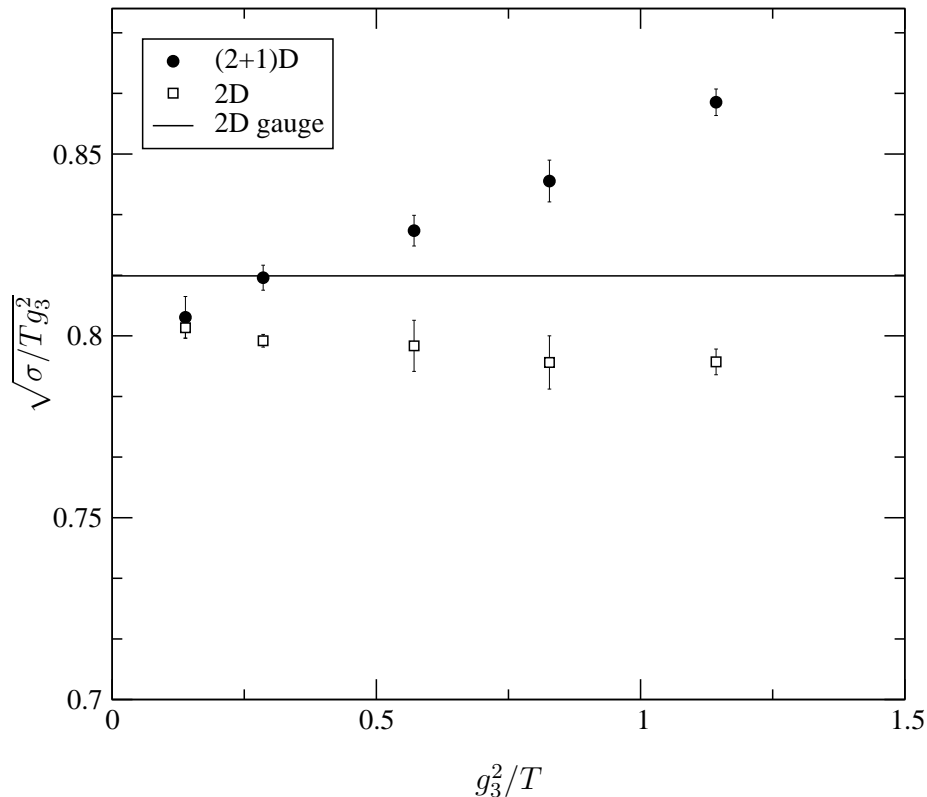


Figure 6: The square root of the physical string tension in units of $g_3\sqrt{T}$ as a function of g_3^2/T in (2+1)D (filled circles) and 2D (squares). The line denotes the scaling limit $\sqrt{2/3}$ in 2D pure gauge theory (54).

can be equivalently rewritten

$$\frac{\sigma_2^0}{g_3^2 T} = \frac{2}{3} + \frac{7}{36} \frac{g_3^2}{T} (aT)^2 + \mathcal{O}\left[\left(\frac{g_3^2}{T}\right)^2 (aT)^4\right], \quad (54)$$

showing that σ_2^0 scales as $2g_3^2 T/3$, up to scaling violations at finite T of order $(aT)^2 = 1/L_0^2$. The quantities reported in Fig. 6 versus g_3^2/T are the values of $\sqrt{\sigma}$ in units of $g_3\sqrt{T}$, which we thus compare to $\sqrt{2/3}$. The numerical values of $\sigma_2^\phi/(g_3^2 T)$ and $\sigma_{2+1}/(g_3^2 T)$ were obtained from the simulations for $L_0=4$. From the 2D point of view, we see that introducing the ϕ field modifies the picture quite weakly: no sizable g_3^2/T dependence around a value close to $\sqrt{2/3}$. The behaviour for σ_{2+1} is substantially different, with a sizable slope in g_3^2/T . The difference observed between σ_{2+1} and σ_2^ϕ may be understood as a consequence of W not being a static operator: the average of its non static modes with the $(2+1)D$ weight are missing in its calculation with the effective action. However, scaling violations may also contribute differently to

these two σ 's, so that definite conclusions require complementary simulations. Let us finally recall that systematic errors can be present in σ measurements, so that we cannot infer from the data presented in Fig. 6 whether or not their infinite T limit is the same, and equal to $2/3$.

5 Conclusion

In this article we have described a detailed investigation of the validity of dimensional reduction for SU(3) gauge theory in 2+1 dimensions at high temperature. We have constructed the reduced model for the static variables in the same way as it was previously done in [6, 7, 8] on the reduction of QCD in 3+1 dimensions. This means that the integration over the non static modes has been performed perturbatively, and the effective couplings have been kept to one loop order for the two point and four point functions. Higher order contributions go to zero at high temperature. Higher derivative couplings are unimportant at large distances.

We investigated the validity of this approximation by calculating the correlation function between Polyakov loops, and the spatial string tension. For the 2+1 dimensional theory and the corresponding 2 dimensional reduced adjoint Higgs-gauge model we were able to obtain very precise numerical results. Therefore we could make a detailed comparison, including a scaling analysis which strongly supports the assumption that our lattices correspond to a large enough value of the temporal extent L_0 .

We have found that for the correlation between Polyakov loops the dimensional reduction works very well down to temperatures $T \approx 1.5T_c$, even at distances down to or below $1/T$. And it does even better than in the 3+1 dimensional case.

The correlation between Polyakov loops is well described by a simple pole in momentum space, even at high temperatures. This is in some contrast to 3+1 dimensional QCD, where at high temperatures the data seem to indicate the presence of a cut, corresponding to the exchange of two Debye screened gluons [33, 21, 24, 34]. The difference may be related to the stronger infrared divergences in 2+1 dimensions, making the simple perturbatively resummed Debye screening picture invalid. A further investigation of this behaviour in 3+1 dimensions, as well as the investigation of other correlation functions in the lower dimensional case would certainly be very interesting.

The spatial Wilson loops in 2+1 dimensions do not correspond to a static operator. However, for the string tension, which is extracted from Wilson loops of extent larger than $1/T$, one can hope that the non static corrections are small. That this is in fact the case is supported by the actual comparison with the two dimensional model. For this operator, the Higgs sector seems to have little influence, and there

is a fairly good agreement also with the pure two dimensional gauge theory, which is analytically solvable, and where confinement is given by the two dimensional Coulomb potential. The differences between the string tension in the three cases considered is a few percent. To judge if these differences are real continuum effects, one must further study finite size and scaling corrections.

Our work shows that it may be possible to explain the non perturbative features of 2+1 dimensional QCD in the deconfined phase with a relatively simple two dimensional model.

Acknowledgments The authors thank Christian Legeland for the use of his 3D SU(3) data and are grateful to Jean-Paul Blaizot for his interest and clarifying comments. P.B. was supported by the Alexander von Humboldt Foundation and partially by the KBN grant 2 P03B 019 17, and T.R. by a Heisenberg fellowship. K.P. was supported by DAAD. We also thank the DFG for support under the contract Ka 1198/4-1. This project was carried out in part on the new cluster computer ALiCE at COMPASS, Wuppertal University, during its initial test phase. We thank the staff of the ALiCE cluster-computer at Compass, University of Wuppertal, for their support.

A Calculation of the ϕ^2 coupling in the Effective 2D Action

We derive the result for h_2 announced in Eq.(25). According to Eqs.(26, 31, 30), the sum we need to perform in the large L_0 limit is

$$W \equiv -\frac{L_0}{3} \tilde{\Pi}_{00}^{ns}(0) = \frac{1}{2} \sum_{n_0=1}^{L_0-1} \frac{dG(x)}{dx}, \quad x = \frac{\pi n_0}{L_0}, \quad (55)$$

$$G(x) = \sin(x) \cos(x) S(\sin^2(x)) \quad (56)$$

$$S(t) \equiv \frac{1}{4\pi^2} \int_{-\pi}^{\pi} \frac{dk_1 dk_2}{2(1+t) - \cos(k_1) - \cos(k_2)}. \quad (57)$$

In the latter integral, we replace the inverse denominator D^{-1} by $\int_0^\infty dy \exp(-yD)$, integrate over k_1, k_2 and use the definition of the modified Bessel function I_0 to get

$$S(t) = \int_0^\infty dy \exp[-2(1+t)y] I_0^2(y). \quad (58)$$

A closed form for this integral is (see for example Eqs.(6.612.4) in [31] and (17.3.9) in [32])

$$S(t) = \frac{(-z)^{1/2}}{2} F(1/2, 1/2; 1; z), \quad z = -\frac{1}{t(t+2)} \quad (59)$$

which relates the behaviour of $S(t)$ at low t to that of the hypergeometric function $F(1/2, 1/2; 1; z)$ at large negative z . One finds (Eq.(15.3.13) of Ref.[32])

$$S(t) = \frac{1}{2\pi^2} \sum_{n=0}^{\infty} \left[\frac{\Gamma(n+1/2)}{\Gamma(n+1)} \right]^2 z^{-n} \left[\log(-z) + 2\Psi(n+1) - 2\Psi(n+1/2) \right]. \quad (60)$$

A first approximation W_0 to W in (55) is obtained from the standard relationship between a sum and an integral:

$$W_0 = \frac{L_0}{2\pi} \int_{\pi/L_0}^{\pi-\pi/L_0} dG(x) + \frac{1}{4} \left[\frac{dG(x)}{dx} \Big|_{x=\frac{\pi}{L_0}} + \frac{dG(x)}{dx} \Big|_{x=\pi-\frac{\pi}{L_0}} \right] \quad (61)$$

$$= -\frac{L_0}{\pi} G\left(\frac{\pi}{L_0}\right) + \frac{1}{2} \frac{dG(x)}{dx} \Big|_{x=\frac{\pi}{L_0}}, \quad (62)$$

where use has been made of the symmetry of $\frac{dG(x)}{dx}$ under $x \leftrightarrow \pi - x$. Up to terms which vanish as $\pi/L_0 \rightarrow 0$, Eq. (60) gives:

$$W_0 \simeq -\frac{1}{2\pi} \left[\frac{3 \log 2}{2} + 1 - \log \pi + \log L_0 \right]. \quad (63)$$

For that part of $G(x)$ which is analytic at $x = 0$, this is the right answer. A correction to the constant term in L_0 however arises from the logarithmic singularity of $G(x)$ (Euler — Mac-Laurin formula, [32]). As $x \rightarrow 0$, we have $\frac{dG}{dx} \simeq -\frac{1}{\pi} \log \frac{n_0}{L_0}$ up to analytic terms, whose contribution W^{log} to W from Eq. (60) can be computed using

$$\sum_{n_0=1}^{L_0/2} \log \frac{n_0}{L_0} = \log \left(\frac{(L_0/2)!}{L_0^{L_0/2}} \right) \simeq \log \frac{\sqrt{\pi L_0}}{(2e)^{L_0/2}} \quad (64)$$

and found to be

$$W^{log} = -\frac{1}{2\pi} \left[\log(2L_0\pi) - L_0(1 + \log 2) \right]. \quad (65)$$

This we compare to the contribution W_0^{log} to W_0 of the same singular part of $\frac{dG}{dx}$, namely

$$W_0^{log} = -\frac{1}{2\pi} \left[\log(2L_0) - L_0(1 + \log 2) \right], \quad (66)$$

so that in the limit $L_0 \rightarrow \infty$ the final result is

$$W = W_0 - W_0^{log} + W^{log} \tag{67}$$

$$= -\frac{1}{2\pi} \left[\frac{5}{2} \log 2 - 1 + \log L_0 \right]. \tag{68}$$

References

- [1] P. Ginsparg, *Nucl. Phys.* **B170** (1980) 388.
- [2] T. Appelquist and R. Pisarski, *Phys. Rev.* **D23** (1981) 2305.
- [3] S. Nadkarni, *Phys. Rev.* **D27** (1983) 917; *Phys. Rev.* **D38** (1988) 3287.
- [4] N. P. Landsman, *Nucl. Phys.* **B322** (1989) 498.
- [5] T. Reisz, *Z. f. Phys.* **C53** (1992) 169.
- [6] P. Lacock, D. E. Miller and T. Reisz, *Nucl. Phys.* **B369** (1992) 501.
- [7] L. Kärkkäinen, P. Lacock, D. E. Miller, B. Petersson and T. Reisz, *Phys. Lett.* **B282** (1992) 121.
- [8] L. Kärkkäinen, P. Lacock, B. Petersson and T. Reisz, *Nucl. Phys.* **B395** (1993) 733.
- [9] P. Lacock, T. Reisz, *Nucl. Phys. B (Proc. Suppl.)* **30** (1993) 307
- [10] K. Kajantie, M. Laine, K. Rummukainen, M. Shaposhnikov, *Phys. Lett* **77** (1996) 2887, *Nucl. Phys.* **B493** (1997) 413.
M. Gurtler, E.-M. Ilgenfritz, A. Schiller, *Phys. Rev.* **D56** (1997) 3888.
F. Karsch, T. Neuhaus, A. Patkos, J. Rank, *Nucl. Phys. Proc. Supl.* **53** (1997) 623.
- [11] K. Kajantie, M. Laine, K. Rummukainen, M. Shaposhnikov, *Nucl. Phys.* **B503** (1997) 357.
- [12] K. Kajantie, M. Laine, A. Rajantie, K. Rummukainen, and M. Tsypin, *JHEP* **9811** (1998) 11.
- [13] K. Kajantie, M. Laine, J. Peisa, A. Rajantie, K. Rummukainen, M. Shaposhnikov *Phys. Rev. Lett.* **79** (1997) 3130.
- [14] S. Datta, S. Gupta, *Nucl. Phys.* **B534** (1998) 392, *Phys.Lett.* **B471** (2000) 382.

- [15] F. Karsch, M. Oevers and P. Petreczky, “Screening masses of hot $SU(2)$ gauge theory from the 3D adjoint Higgs model”, hep-ph/9902373.
- [16] A. Hart and O. Philipsen, “The spectrum of the three-dimensional adjoint Higgs model and hot $SU(2)$ gauge theory,”, hep-lat/9908041.
- [17] L. Kärkkäinen, P. Lacock, D.E. Miller, B. Petersson, T. Reisz *Phys. Lett.* **B312** (1993) 173.
- [18] G.S. Bali, J. Fingberg, U.M. Heller, F. Karsch and K. Schilling, *Phys. Rev. Lett.* **71** (1993) 3059
F. Karsch, E. Laermann, M. Lütgemeier *Phys. Lett.* B346 (1995) 94.
- [19] E. D’Hoker, *Nucl. Phys* **B201** (1982) 401.
- [20] C. Legeland, *PhD. Thesis*, “Aspects of $(2+1)$ Dimensional Lattice Gauge Theory” (University of Bielefeld, Germany, September 1998).
- [21] B. Petersson and T. Reisz, *Nucl. Phys.* **B353** (1991) 757.
- [22] C. Curci and P. Menotti, *Z. f. Phys.* **C21** (1984) 281; C. Curci, P. Menotti and G. Paffuti, *Z. f. Phys.* **C26** (1985) 549.
- [23] T. Reisz, *Jour. Math. Phys.* **32** (1991) 515
- [24] A. Irbäck, P. Lacock, D. Miller, B. Petersson, T. Reisz, *Nucl. Phys.* **B363** (1991) 34.
- [25] L. Kärkkäinen, P. Lacock, D.E. Miller, B. Petersson and T. Reisz, *Nucl. Phys.* **B418** (1994) 3.
- [26] T. Reisz, “Dimensionally Reduced $SU(2)$ Yang-Mills Theory is Confined”, in *Quantum Field Theoretical Aspects of High Energy Physics*, 230-235, B. Geyer and E.M. Ilgenfritz Eds., Frankenhausen 1993.
- [27] N. Cabibbo and E. Marinari, *Phys. Lett.* **B119** (1982) 387.
- [28] A. D. Kennedy and B. J. Pendleton, *Phys. Lett.* **B156** (1985) 393.
- [29] D. J. Gross and E. Witten, *Phys. Rev.* **D21** (1980) 446.
- [30] C. B. Lang, P. Salomonson and B. S. Skagerstam, *Phys. Letters* **100** (1981) 29.
- [31] I.S. Gradshteyn and I.M. Ryzhik, *Table of Integrals, Series, and Products*, Alan Jeffrey, Ed. (Academic Press).

- [32] M. Abramowitz and I.A. Stegun, Handbook of Mathematical Functions, (National Bureau of Standards).
- [33] M. Gao, Phys. Rev. **D40** (1989) 2708.
- [34] O. Kaczmarek, F. Karsch, E. Laermann and M. Lutgemeier, “Heavy quark potentials in quenched QCD at high temperature,” hep-lat/9908010.